Chemical Communications

c9cc07750b

We have presented the Graphical Abstract text and image for your article below. This brief summary of your work will appear in the contents pages of the issue in which your article appears.

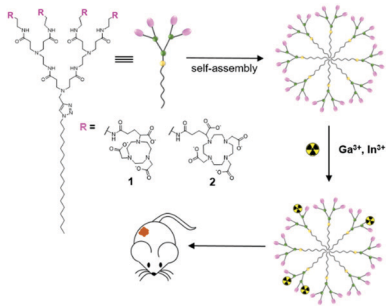

A self-assembling amphiphilic dendrimer nanotracer for SPECT imaging Q2

Ling Ding, Zhenbin Lyu, Aura Tintaru, Erik Laurini, Domenico Marson, Beatrice Louis, Ahlem Bouhlel, Laure Balasse, Samantha Fernandez, Philippe Garrigue, Eric Mas, Suzanne Giorgio, Sabrina Pricl, Benjamin Guillet and Ling Peng*

Bioimaging has revolutionized modern medicine, and nanotechnology can offer further specific and sensitive imaging. Q3

Please check this proof carefully. Our staff will not read it in detail after you have returned it.

Please send your corrections either as a copy of the proof PDF with electronic notes attached or as a list of corrections. **Do not edit the text within the PDF or send a revised manuscript** as we will not be able to apply your corrections. Corrections at this stage should be minor and not involve extensive changes.

Proof corrections must be returned as a single set of corrections, approved by all co-authors. No further corrections can be made after you have submitted your proof corrections as we will publish your article online as soon as possible after they are received.

Please ensure that:

- The spelling and format of all author names and affiliations are checked carefully. You can check how we have identified the authors' first and last names in the researcher information table on the next page. **Names will be indexed and cited as shown on the proof, so these must be correct.**
- Any funding bodies have been acknowledged appropriately and included both in the paper and in the funder information table on the next page.
- All of the editor's queries are answered.
- Any necessary attachments, such as updated images or ESI files, are provided.

Translation errors can occur during conversion to typesetting systems so you need to read the whole proof. In particular please check tables, equations, numerical data, figures and graphics, and references carefully.

Please return your **final** corrections, where possible within **48 hours** of receipt, by e-mail to: chemcomm@rsc.org. If you require more time, please notify us by email.

Funding information

Providing accurate funding information will enable us to help you comply with your funders' reporting mandates. Clear acknowledgement of funder support is an important consideration in funding evaluation and can increase your chances of securing funding in the future.

We work closely with Crossref to make your research discoverable through the Funding Data search tool (http://search.crossref.org/funding). Funding Data provides a reliable way to track the impact of the work that funders support. Accurate funder information will also help us (i) identify articles that are mandated to be deposited in **PubMed Central (PMC)** and deposit these on your behalf, and (ii) identify articles funded as part of the **CHORUS** initiative and display the Accepted Manuscript on our web site after an embargo period of 12 months.

Further information can be found on our webpage (http://rsc.li/funding-info).

What we do with funding information

We have combined the information you gave us on submission with the information in your acknowledgements. This will help ensure the funding information is as complete as possible and matches funders listed in the Crossref Funder Registry.

If a funding organisation you included in your acknowledgements or on submission of your article is not currently listed in the registry it will not appear in the table on this page. We can only deposit data if funders are already listed in the Crossref Funder Registry, but we will pass all funding information on to Crossref so that additional funders can be included in future.

Please check your funding information

The table below contains the information we will share with Crossref so that your article can be found *via* the Funding Data search tool. **Please check that the funder names and grant numbers in the table are correct and indicate if any changes are necessary to the Acknowledgements text.**

Funder name	Funder's main country of origin	Funder ID (for RSC use only)	Award/grant number
Ligue Contre le Cancer	France	501100004099	LP, ZL
China Scholarship Council	China	501100004543	Unassigned
Associazione Italiana per la Ricerca sul Cancro	Italy	501100005010	IG17413
European Cooperation in Science and Technology	European Union	501100000921	CA 17140
Horizon 2020 Framework Programme	European Union	100010661	Unassigned

Q1

Researcher information

Please check that the researcher information in the table below is correct, including the spelling and formatting of all author names, and that the authors' first, middle and last names have been correctly identified. **Names will be indexed and cited as shown on the proof, so these must be correct.**

If any authors have ORCID or ResearcherID details that are not listed below, please provide these with your proof corrections. Please ensure that the ORCID and ResearcherID details listed below have been assigned to the correct author. Authors should have their own unique ORCID iD and should not use another researcher's, as errors will delay publication.

Please also update your account on our online manuscript submission system to add your ORCID details, which will then be automatically included in all future submissions. See here for step-by-step instructions and more information on author identifiers.

First (given) and middle name(s)	Last (family) name(s)	ResearcherID	ORCID iD
Ling	Ding		
Zhenbin	Lyu		
Aura	Tintaru		
Erik	Laurini		0000-0001-6092-6532
Domenico	Marson	G-7162-2012	0000-0003-1839-9868
Beatrice	Louis		
Ahlem	Bouhlel		

Laure	Balasse		
Samantha	Fernandez		
Philippe	Garrigue		
Eric	Mas		
Suzanne	Giorgio		
Sabrina	Pricl	M-7493-2015	0000-0001-8380-4474
Benjamin	Guillet		
Ling	Peng		0000-0003-3990-5248

Queries for the attention of the authors

Journal: **ChemComm**

Paper: **c9cc07750b**

Title: **A self-assembling amphiphilic dendrimer nanotracer for SPECT imaging**

For your information: You can cite this article before you receive notification of the page numbers by using the following format: (authors), Chem. Commun., (year), DOI: 10.1039/c9cc07750b.

Editor's queries are marked on your proof like this Q1, Q2, etc. and for your convenience line numbers are indicated like this 5, 10, 15, ...

Please ensure that all queries are answered when returning your proof corrections so that publication of your article is not delayed.

Query reference	Query	Remarks
Q1	Funder details have been incorporated in the funder table using information provided in the article text. Please check that the funder information in the table is correct.	
Q2	Please confirm that the spelling and format of all author names is correct. Names will be indexed and cited as shown on the proof, so these must be correct. No late corrections can be made.	
Q3	Please check that the inserted Graphical Abstract image and text are suitable. If you provide replacement text, please ensure that it is no longer than 250 characters (including spaces).	

ChemComm

COMMUNICATION

A self-assembling amphiphilic dendrimer nanotracer for SPECT imaging†

Cite this: DOI: 10.1039/c9cc07750b

Received 2nd October 2019,
Accepted 20th November 2019

DOI: 10.1039/c9cc07750b

rsc.li/chemcomm

Ling Ding,[ab] Zhenbin Lyu,[a] Aura Tintaru,[c] Erik Laurini,[d] Domenico Marson,[d] Beatrice Louis,[ef] Ahlem Bouhlel,[ef] Laure Balasse,[ef] Samantha Fernandez,[ef] Philippe Garrigue,[ef] Eric Mas,[g] Suzanne Giorgio,[a] Sabrina Pricl,[dh] Benjamin Guillet[ef] and Ling Peng *[a]

Bioimaging has revolutionized modern medicine, and nanotechnology can offer further specific and sensitive imaging. We report here an amphiphilic dendrimer able to self-assemble into supramolecular nanomicelles for effective tumor detection using SPECT radioimaging. This highlights the promising potential of supramolecular dendrimer platforms for biomedical imaging.

Medical imaging plays an important role in modern medicine by providing accurate information relating to diagnosing, grading and staging diseases as well as monitoring treatment response and efficacy.[1] Among the commonly used non-invasive imaging modalities such as magnetic resonance imaging (MRI), computed tomography (CT), positron emission tomography (PET), single photon emission computed tomography (SPECT), and ultrasonography (US), PET and SPECT have the highest sensitivity, and are able to visualize functional information quantitatively, which is very important for disease assessment and diagnosis and personalized medicine.[1–5] Nanotechnology can further enhance the sensitivity and specificity of molecular imaging *via* the "Enhanced Permeation and Retention (EPR)" effect (also named passive tumor targeting).[6–8] EPR results in nanoparticle specific tumor accumulation thanks to the leaky vasculature and dysfunctional lymphatic system characterizing the tumor microenvironment.[9] In addition, nanosystems carrying and incorporating abundant imaging reporters can significantly amplify the contrast signal for better imaging and diagnosis. Consequently, a myriad of nanosystems have been explored for PET and SPECT imaging of tumors.[2,6,10]

We have recently used the self-assembling amphiphilic dendrimer **Ga-1** to establish an innovative nanotracer for PET imaging (Fig. 1).[11] This dendrimer is composed of a long hydrophobic alkyl chain and a hydrophilic poly(amidoamine) (PAMAM) dendron bearing the PET radionuclide ^{68}Ga(III) complexed within the macrocyclic chelator NOTA (1,4,7-triazacyclononane-1,4,7-triacetic acid) at the peripheral units (**Ga-1** in Fig. 1). It self-assembles into small and stable nanomicelles, which can effectively accumulate in tumors. These nanomicelles deliver excellent results in PET imaging of different tumors, including some which could not be detected with the standard clinical PET agent [^{18}F]FDG (2-fluorodeoxyglucose).[11] The performance of this dendrimer radiotracer is largely ascribed to the

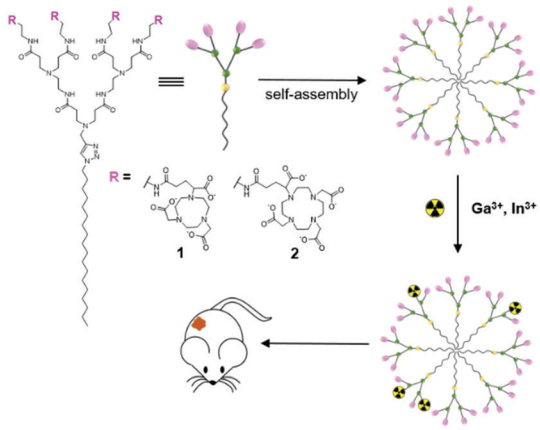

Fig. 1 Self-assembling dendrimer nanosystems based on the amphiphilic dendrimers **1** and **2** bearing radionuclide, for positron emission tomography (PET) and single photon emission computed tomography (SPECT) imaging of tumors, respectively.

[a] *Aix Marseille Univ, CNRS, Centre Interdisciplinaire de Nanoscience de Marseille (UMR 7325), Equipe Labellisée Ligue Contre le Cancer, Marseille, France. E-mail: ling.peng@univ-amu.fr*
[b] *Aix Marseille Univ, CNRS, CRMBM, Marseille, France*
[c] *Aix Marseille Univ, CNRS, Institut de Chimie Radicalaire (UMR7273), Marseille, France*
[d] *Molecular Biology and Nanotechnology Laboratory (MolBNL@UniTS), DEA, University of Trieste, Trieste, Italy*
[e] *Aix Marseille Univ, INSERM, INRA, C2VN, Marseille, France*
[f] *Aix Marseille Univ, CNRS, Centre Européen de Recherche en Imagerie Médicale (CERIMED), Marseille, France*
[g] *Aix Marseille Univ, CNRS, INSERM, Institut Paoli-Calmettes, Centre de Recherche en Cancérologie de Marseille (CRCM), Marseille, France*
[h] *Department of General Biophysics, Faculty of Biology and Environmental Protection, University of Lodz, Lodz, Poland*

† Electronic supplementary information (ESI) available. See DOI: 10.1039/c9cc07750b

beneficial combination of its unique multivalent dendrimeric structure and the relevant EPR effect.

Motivated by the promising PET imaging results,[11] we aimed at further exploiting self-assembling nanotechnology for constructing effective dendrimer-based radiotracers for SPECT imaging. Different from PET, SPECT has the capacity to image multiple processes simultaneously by using the corresponding detection windows of different radionuclides with distinct gamma ray energies.[1–3] In addition, SPECT is more readily accessible and less expensive than PET in the clinics, even if PET has higher sensitivity and resolution. Recent progress in advanced detection technology and the combination with computed tomography (CT) has considerably improved the resolution and sensitivity of SPECT, placing SPECT as a quantitative imaging modality similar to PET.[3,12] Also, SPECT radiotracers generally have longer half-lives, which allows the characterization of slow kinetic processes and long biological events that take hours or days. Common radionuclides used in SPECT imaging include technetium-99m ([^{99m}Tc]Tc), indium-111 ([^{111}In]In) and iodine-123 ([^{123}I]I). Although [^{99m}Tc]Tc is the most widely used, [^{111}In]In has a relatively longer half-life (2.8 days). Accordingly, in this study, we chose [^{111}In]In as the radionuclide to develop a dendrimer radiotracer for SPECT imaging with the aim of monitoring and measuring long and slow biological processes such as tumor development and treatment.

Chelation of $^{111}In^{3+}$ to a thermodynamically stable and kinetically inert complex is a fundamental requirement for SPECT imaging in order to prevent the release of free radionuclide.[4,5] The cyclic chelator DOTA (1,4,7,10-tetraazacyclododecane-1,4,7,10-tetraacetic acid) and the acyclic chelator DTPA (diethylenetriaminepentaacetic acid) are the most frequently used in nuclear medicine.[13] In general, DOTA forms more stable complexes with radionuclide ions than the acyclic chelator DTPA because of the entropically favorable preorganized and rigid binding sites within the DOTA ring. Nevertheless, the process of metal-complex formation is often slow for DOTA, and requires high temperature and long reaction times. Yet, as DOTA is the "gold standard" chelator for $^{111}In^{3+}$,[13] and on the basis of our previous experience in developing the NOTA-conjugated dendrimer to complex with the radionuclide Ga^{3+} (**Ga-1**) for PET imaging (Fig. 1),[11] we selected DOTA as the chelator to construct the amphiphilic dendrimer **2** which, in turn, was complexed with $^{111}In^{3+}$ to generate **In-2** for SPECT imaging (Fig. 1 and 2). Knowing that the DOTA ring is considerably larger than that of NOTA, we initially worried about the eventual synthetic difficulty stemming from steric hindrance of the DOTA terminals in **2**. Gratifyingly, we could reliably synthesize the DOTA-conjugated dendrimer **2** with high yield (Fig. 2A). Also of note, we successfully prepared the stable dendrimer complex **In-2** at

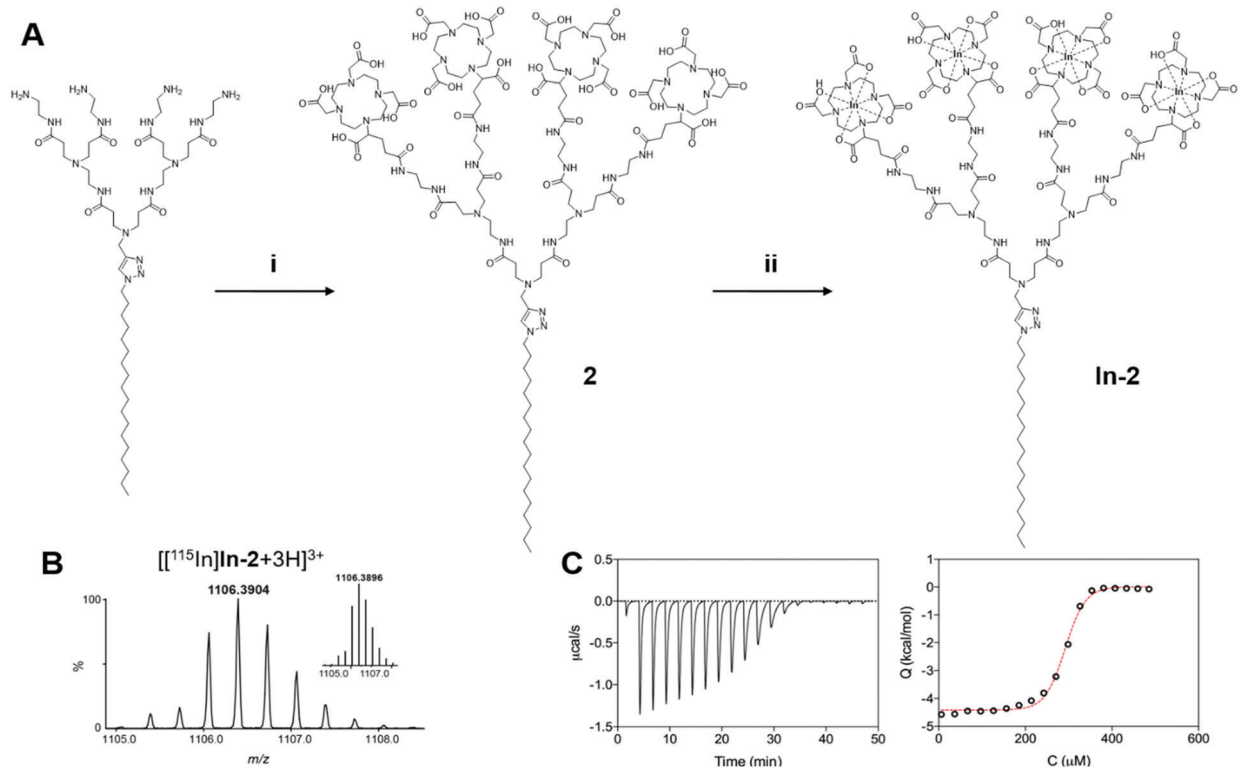

Fig. 2 Synthesis of the amphiphilic dendrimer **2** bearing DOTA units and its chelation with the nonradioactive isotope [^{115}In]In^{3+} at the terminals to deliver the dendrimer **In-2**. (A) Synthesis scheme: (i) (a) DOTA-GA(tBu)$_4$, PyBOP, NMM, DMF, 30 °C, 72 h; (b) TFA, CH_2Cl_2, 30 °C, 24 h. (ii) [^{115}In]$InCl_3$, 1.0 M HCl, 37 °C, 2 h. (B) High-resolution mass spectrum (HRMS) showing the isotopic pattern of the observed triply charged species [[^{115}In]**In-2** + 3H]$^{3+}$. The inset shows the calculated isotopic pattern. (C) Isothermal titration calorimetry (ITC) curve (right) for chelation of In^{3+} with the dendrimer **2**. The left panel shows measured heat power *versus* time elapsed during titration.

37 °C within 2 hours. Importantly, **In-2** self-assembled into small and uniform nanomicelles for effective SPECT imaging of tumors. We present below the synthesis and characterization of the amphiphilic dendrimer **2** and its complex with In^{3+} as well as the nanomicelles formed with the obtained dendrimer **In-2** for SPECT imaging.

Similar to our previous synthesis of the NOTA-dendrimer **1**,[11] we conjugated the amine-terminated amphiphilic dendrimer with the reagent DOTA-GA(tBu)$_4$, followed by deprotection for preparing **2** (Fig. 2A). Compared to the synthesis of **1**, we halved the quantity of the reagent DOTA-GA(tBu)$_4$ from 4 to 2 equivalents, which considerably simplified the purification procedure while maintaining the high synthesis yield of 88% for **2**. The chemical structure and integrity of **2** was analyzed and confirmed using ^{1}H, ^{13}C and 2D NMR and high-resolution mass spectrometry (HRMS), which exhibited the signals characteristic of the chemically conjugated DOTA groups (Fig. S1 and S2, ESI†). Chelation of the stable isotope $^{115}In^{3+}$ by **2** was performed using $^{115}InCl_3$ at 37 °C, pH 5.0 for 2 hours (Fig. 2A), and the final dendrimer **In-2** was obtained in pure form as a white solid after dialysis to remove the free $^{115}In^{3+}$. The successful complexation of four $^{115}In^{3+}$ by each molecule of the dendrimer **2** was confirmed using HRMS, which showed the isotopic pattern characteristic of the triply charged species [^{115}**In-2** + 3H]$^{3+}$ in addition to the expected molecular weight peak (Fig. 2B and Fig. S3B, ESI†).[14] It is important to mention that the formation of DOTA complexes with metal ions usually requires high temperature at 95 °C and long reaction time of several hours because of the slow binding kinetics of DOTA. Remarkably, we successfully chelated In^{3+} with the DOTA-conjugated dendrimer **2** at relatively low temperature (37 °C) within 2 h. This may be ascribed to the steric congestion created at the dendrimer terminals,[15] making the DOTA entities in **2** more reactive and hence favorably promoting their complexation with In^{3+} rapidly and at lower temperature to form the stable complex **In-2**.

To corroborate the reliable synthesis of **In-2**, we studied the formation of the complex between dendrimer **2** and In^{3+} using isothermal titration calorimetry (ITC). Specifically, a solution of **2** at 100 μM was titrated with the solution of $InCl_3$ at pH = 5 and 37 °C (see the ESI† for details). The left panel in Fig. 2C shows that the interaction between the DOTA cages of **2** and the In^{3+} cations is characterized by a robust exothermic behavior, reflecting an enthalpy-driven binding process ($\Delta H = -5.25$ kcal mol^{-1}) led by strong coordination interactions between the In^{3+} and the DOTA cages of **2**. Notably, the entropic component ($-T\Delta S = -2.61$ kcal mol^{-1}) also favors the stability of **In-2**. This is probably due to a synergistic effect of the hydrophobic interactions between the apolar dendrimer tails, which aggregate together with the concomitant release of water and ions from the charged surfaces when they form complexes with the cations. Accordingly, the spontaneous formation of the **In-2** complex is highly thermodynamically favorable, with a Gibbs free energy (ΔG) value of −7.86 kcal mol^{-1}. Interestingly, ITC measurements show that the number of $^{115}In^{3+}$ in **In-2** is 4.02, which confirms the ideal stoichiometry of 4 : 1. Taken together, the ITC results provide evidence that the synthesis of **In-2** was successful, and that **In-2** is a stable complex.

We next studied the self-assembly of **In-2** in solution. **In-2** spontaneously self-assembled into small and spherical nanoparticles with average dimensions around 18 nm, as revealed by transmission electron microscopy (TEM) (Fig. 3A). Also, dynamic light scattering (DLS) analysis confirmed the formation of small nanoparticles with sizes around 19 nm, which is typical for nanomicelles (Fig. 3B). The formed nanoparticles were stable, with the critical micelle concentration (CMC) being 60 ± 10 μM (Fig. S4, ESI†). Further molecular dynamics (MD) simulations confirmed the spontaneous aggregation of **In-2** into spherical micelles. Fig. 3C illustrates a representative configuration of the stable **In-2** micelles obtained at the end of the computational process starting from a random distribution of **In-2** in solution. The calculated average micelle diameter was around 15 nm, in close agreement with the values obtained using experimental techniques (TEM and DLS). Along the entire MD trajectories, all the In^{3+}/DOTA terminal groups were nicely located at the micellar periphery without any back-folding observed, as evident from the relevant radial distribution function of the terminal groups shown in Fig. 3D.

Encouraged by the favorable self-assembly properties of **In-2**, we prepared the corresponding radioactive dendrimer complex [^{111}In]**In-2** for SPECT imaging. We obtained the [^{111}In]**In-2** complex with a satisfying radiochemical purity over 91 ± 2% along with a high molar activity of 1.09 ± 0.15 GBq μmol^{-1}. In addition, this radiochemical purity and integrity was maintained for up to 30 hours at 37 °C in human serum

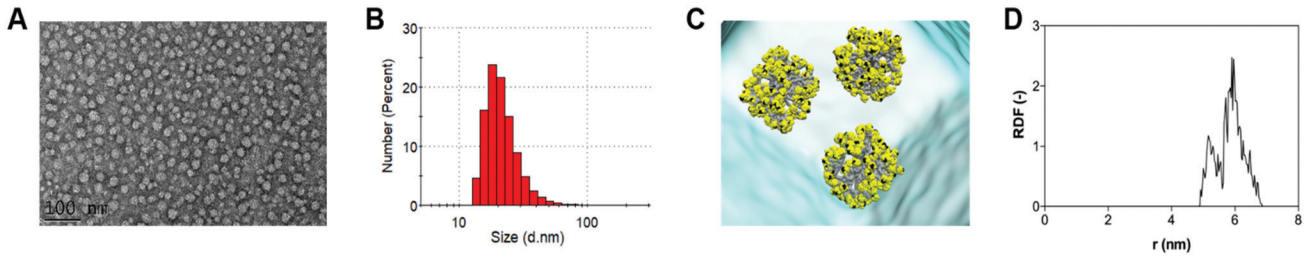

Fig. 3 Self-assembling of the amphiphilic dendrimer **In-2** into small and uniform nanomicelles. (A) Transmission electron microscopy (TEM) image, (B) dynamic light scattering (DLS) measurement, and (C and D) computer modeling of the self-assembled nanoparticles formed by **In-2**. (C) Final image of the **In-2** self-assembly process into spherical micelles as obtained from atomistic molecular dynamics (MD) simulations. The different parts of the **In-2** molecules are represented as spheres (atom color: grey, hydrocarbon chain; yellow, DOTA cage; black, In^{3+}), while water molecules are shown as aqua transparent spheres. ~~The first water shell surrounding each molecule/micelle is highlighted as a light cyan transparent contour.~~ (D) Radial distribution function of the In(III)-bearing terminals as a function of the distance from the center of mass of the **In-2** micelles.

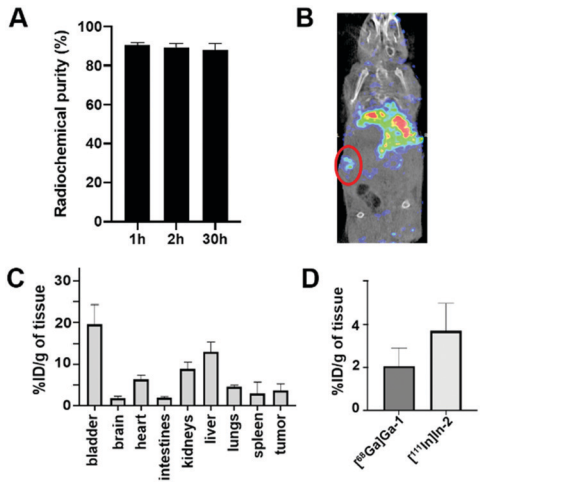

Fig. 4 Radiolabeled dendrimer [^{111}In]**In-2** for SPECT imaging in a mouse orthotopic xenograft model of pancreatic adenocarcinoma (SOJ-6 cell line). (A) [^{111}In]**In-2** radiochemical purity and stability in human serum at 37 °C for at least 30 h was assessed by radio-thin layer chromatography. (B) Representative μSPECT/CT image of [^{111}In]**In-2** 180 minutes after intravenous injection. Orthotopic SOJ6 tumor is highlighted by the red circle (n = 3 mice). (C) Biodistribution of [^{111}In]**In-2** quantified in each organ by μSPECT/CT 180 min after injection. Results are expressed as the mean percentage of injected dose per gram of tissue (n = 3 mice). (D) Tumor uptake comparison between [^{68}Ga]**Ga-1** and [^{111}In]**In-2** in the same mice (n = 3).

(Fig. 4A). On the basis of the high radiochemical purity and stability, we performed SPECT imaging using [^{111}In]**In-2** in orthotopically xenografted mice bearing tumors derived from a human pancreatic adenocarcinoma tumor cell line, SOJ-6 (Fig. 4B). Co-registration with CT enabled precise, anatomical localization of SPECT signals for further quantification. The biodistribution of [^{111}In]**In-2** mapped by SPECT has obvious similarities with that obtained with [^{68}Ga]**Ga-1** using PET (Fig. 4B and Fig. S4, ESI†).[11] [^{111}In]**In-2** showed hepatic retention and elimination through the urinary tract (Fig. 4C and Fig. S4B, ESI†), similar to what was observed for [^{68}Ga]**Ga-1** using PET,[11] and many other nanoparticles.[2,6–8] Notably, the hepatic uptake of [^{111}In]**In-2** was 2-fold higher than we previously observed for [^{68}Ga]**Ga-1**, along with a higher kidney retention (Fig. S4B, ESI†). The tumor uptake of [^{111}In]**In-2** was almost 2-fold higher than that of [^{68}Ga]**Ga-1** (Fig. 4D and Fig. S4, ESI†), and the duration of the signal was also more stable and longer. This difference may stem from the different chelators, and the resulting negatively charged [^{111}In]**In-2** and neutral [^{68}Ga]**Ga-1**, as well as the slightly different size of [^{111}In]**In-2** and neutral [^{68}Ga]**Ga-1**. In addition, [^{111}In]In has a longer half-life than [^{68}Ga]Ga. Altogether, these results confirm the high flexibility and modularity of our dendrimer nanosystems for bioimaging.

In conclusion, we have developed a supramolecular dendrimer nanosystem based on self-assembly of the amphiphilic dendrimer **In-2** for SPECT imaging in an orthotopic tumor-xenograft mouse model. The work present here alongside our previous studies on PET imaging[11] and drug delivery,[16–18] highlights that nanosystems formed from self-assembling dendrimers have great potential as novel and robust platforms for various biomedical applications. The supramolecular dendrimer nanosystem developed in this work can be further extended to radiotherapy, and to applications which combine radiotherapy and imaging,[4,5] for example, those using the radionuclide [^{177}Lu]Lu. We are working actively to realize these exciting possibilities.

We thank Michel Skandalovski (CERIMED, Aix-Marseille University) and Sandrine Pons (Faculty of Pharmacy, Aix-Marseille University) for technical support. This work was supported by the Ligue Nationale Contre le Cancer (LP, ZL), the ERA-Net EURONANOMED projects ''Target4Cancer'', ''NANOGLIO'' and ''TARBRAINFECT'' (LP), H2020 NMBP ''SAFE-N-MEDTECH'' (LP), China Scholarship Council (LD) and Italian Association for Cancer Research (IG17413) (SP). This article is based on work from COST Action CA 17140 ''Cancer Nanomedicine from the Bench to the Bedside'' supported by COST (European Cooperation in Science and Technology).

Conflicts of interest

There are no conflicts to declare.

Notes and references

1 M. L. James and S. S. Gambhir, *Physiol. Rev.*, 2012, **92**, 897–965.
2 D. Ni, E. B. Ehlerding and W. Cai, *Angew. Chem., Int. Ed.*, 2019, **58**, 2570–2579.
3 O. Israel, O. Pellet, L. Biassoni, D. De Palma, E. Estrada-Lobato, G. Gnanasegaran, T. Kuwert, C. la Fougère, G. Mariani, S. Massalha, D. Paez and F. Giammarile, *Eur. J. Nucl. Med. Mol. Imaging*, 2019, **46**, 1990–2012.
4 T. J. Wadas, E. H. Wong, G. R. Weisman and C. J. Anderson, *Chem. Rev.*, 2010, **110**, 2858–2902.
5 T. I. Kostelnik and C. Orvig, *Chem. Rev.*, 2019, **119**, 902–956.
6 H. Chen, W. Zhang, G. Zhu, J. Xie and X. Chen, *Nat. Rev. Mater.*, 2017, **2**, 17024.
7 C. Li, *Nat. Mater.*, 2014, **13**, 110.
8 E. K.-H. Chow and D. Ho, *Sci. Transl. Med.*, 2013, **5**, 216rv214.
9 H. Maeda, J. Wu, T. Sawa, Y. Matsumura and K. Hori, *J. Controlled Release*, 2000, **65**, 271–284.
10 E.-K. Lim, T. Kim, S. Paik, S. Haam, Y.-M. Huh and K. Lee, *Chem. Rev.*, 2015, **115**, 327–394.
11 P. Garrigue, J. Tang, L. Ding, A. Bouhlel, A. Tintaru, E. Laurini, Y. Huang, Z. Lyu, M. Zhang, S. Fernandez, L. Balasse, W. Lan, E. Mas, D. Marson, Y. Weng, X. Liu, S. Giorgio, J. Iovanna, S. Pricl, B. Guillet and L. Peng, *Proc. Natl. Acad. Sci. U. S. A.*, 2018, **115**, 11454–11459.
12 D. L. Bailey and K. P. Willowson, *Eur. J. Nucl. Med. Mol. Imaging*, 2014, **41**, 17–25.
13 E. W. Price and C. Orvig, *Chem. Soc. Rev.*, 2014, **43**, 260–290.
14 We were unable to obtain well-resolved NMR spectra for In-2 because of the highly quadrupolar effect of the 115In nucleus. For details, please see, *Handbook of High Resolution Multinuclear NMR*, ed. C. Brevard and P. Granger, John Wiley and Sons, Inc., 1981.
15 Z. Zhou, M. Cong, M. Li, A. Tintaru, J. Li, J. Yao, Y. Xia and L. Peng, *Chem. Commun.*, 2018, **54**, 5956–5959.
16 T. Wei, C. Chen, J. Liu, C. Liu, P. Posocco, X. Liu, Q. Cheng, S. Huo, Z. Liang, M. Fermeglia, S. Pricl, X.-J. Liang, P. Rocchi and L. Peng, *Proc. Natl. Acad. Sci. U. S. A.*, 2015, **112**, 2978–2983.
17 C. Chen, P. Posocco, X. Liu, Q. Cheng, E. Laurini, J. Zhou, C. Liu, Y. Wang, J. Tang, V. D. Col, T. Yu, S. Giorgio, M. Fermeglia, F. Qu, Z. Liang, J. J. Rossi, M. Liu, P. Rocchi, S. Pricl and L. Peng, *Small*, 2016, **12**, 3667–3676.
18 Y. Dong, T. Yu, L. Ding, E. Laurini, Y. Huang, M. Zhang, Y. Weng, S. Lin, P. Chen, D. Marson, Y. Jiang, S. Giorgio, S. Pricl, X. Liu, P. Rocchi and L. Peng, *J. Am. Chem. Soc.*, 2018, **140**, 16264–16274.

